

Estimation of ^{239}Pu partial fission cross sections between 5 and 30 MeV

B. Morillon,^{*} B. Mauss, P. Romain, and J. Taieb

CEA, DAM, DIF, F-91297 Arpajon, France and Université Paris-Saclay, CEA, LMCE, 91680 Bruyères-le-Châtel, France



(Received 8 December 2023; accepted 24 May 2024; published 14 June 2024)

Numerous measurements of ^{239}Pu fission cross sections are available for incident neutron energies below 30 MeV. On the other hand, there are no measurements of partial fission cross sections. We propose, in this paper, to give an estimate of these cross sections between 5 and 30 MeV from measurements and calculations of prompt fission neutron spectra and multiplicities. These new cross sections provide a better description of experimental prompt neutron data.

DOI: [10.1103/PhysRevC.109.064613](https://doi.org/10.1103/PhysRevC.109.064613)

I. ^{239}Pu FISSION CROSS SECTION

The ^{239}Pu fission cross section is measured for neutron energies between 10^{-3} eV and 200 MeV. The work of the evaluator is to provide a representation not only of these measurements, but also of all other cross sections for nuclear power applications. To this end, the evaluator is looking for models from nuclear physics to accurately represent the experimental fission data. First and foremost, he determines the first-chance fission, which is the only fission process present for neutrons with an energy below 5 MeV. The ^{240}Pu fission model used to calculate the fission cross section has parameters that are tuned to closely reproduce the measurements. With the same model, the evaluator strives to reproduce the ^{240}Pu fission cross section induced by photons in order to specify the parameters more precisely. Then, from 5-MeV incident energy, second-chance fission opens (the ^{240}Pu compound nucleus emits a neutron and the ^{239}Pu residual nucleus fissions) and finds itself in competition with first-chance fission. Just like first-chance fission, the evaluator adjusts the ^{239}Pu fission parameters to well reproduce the total fission cross section. There is, however, an important difference with the work carried out below 5 MeV. Beyond 5 MeV, the fission cross section measured is the sum of first- and second-chance fission and the evaluator does not know what the proportion of one and the other is. It will become more complicated with the emergence of third-chance fission around 10 MeV (^{238}Pu fission), then fourth- and fifth-chance fission. The evaluator, aware of this indeterminacy, has long been looking for a way to determine the proportion of multichance fission cross sections. Recently, for the first time, Fraïsse *et al.* [1] provide an indirect measurement of the second-chance partial fission probability up to 12 MeV.

We propose in this paper to show how the ^{239}Pu partial fission cross sections can be estimated between 5 and 30 MeV. To that aim, we are looking for partial fission cross sections that allow us to calculate prompt fission neutrons spectra and multiplicities in better agreement with measurements. All the other ingredients of the various models

will be the same as those used to build the ^{239}Pu evaluation file for the JEFF3.3 library [2] released in 2017. The only degree of freedom lies in the partial fission cross sections themselves we want to determine. We must therefore bear in mind that our estimates of fission cross sections depend on the ingredients of the nuclear physics models used.

We will use two methods to estimate these cross sections, both based on the comparison of measurements and calculations with the Madland-Nix model [3] and the Hauser-Feshbach formalism [4]. We will compare our estimates with Fraïsse's data and show the improvements that have been made in the description of prompt fission neutron measurements.

II. MEASUREMENTS OF ^{239}Pu PROMPT FISSION NEUTRONS

The measurements of the spectra [5] as well as the multiplicities [6] of ^{239}Pu prompt fission neutrons, are essential to estimate the proportions of the multichance fission cross sections. They were carried out by the DOE/NNSA CEA-DAM collaboration between the US Department of Energy - National Nuclear Security Administration (DOE/NNSA) and the French Commissariat à l'Énergie Atomique et aux énergies alternatives - Direction des Applications Militaires (CEA-DAM). For incident neutron energies between 1 and 700 MeV, these spectra have been accurately measured with prompt neutrons measured between 200 keV and 12 MeV. Regarding the mean kinetic energy of prompt fission neutrons, it was with prompt neutrons measured between 200 keV and 15 MeV. As this quantity is sensitive to the low-energy part of the spectrum, the authors [5] extrapolated the spectrum below 200 keV using a Maxwell-type distribution. The experimental mean energy is represented in Fig. 1 by the black symbols for incident neutron energy between 1 and 30 MeV. The mean energy increases linearly between 1 and 5 MeV and then drops sharply to an energy of 7.5 MeV to increase again. There is another mean energy drop, but this time of lower amplitude, around 13 MeV. It is mainly these variations in the mean energy that will make it possible to estimate the proportions of

^{*}Contact author: benjamin.morillon@cea.fr

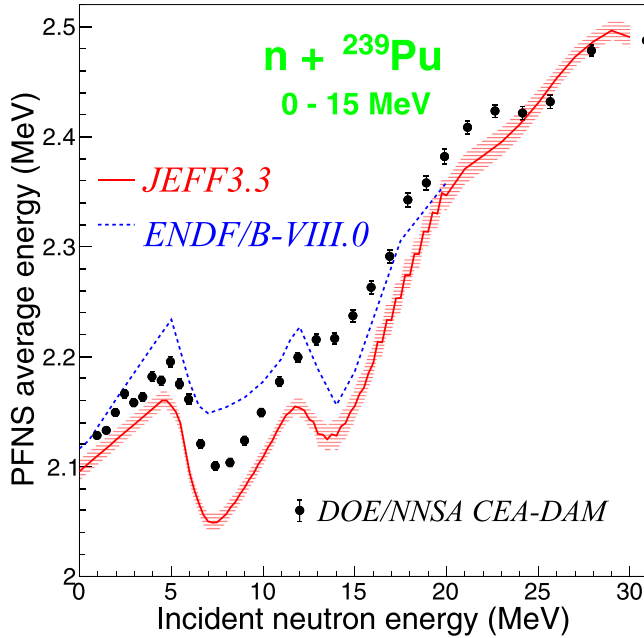


FIG. 1. ^{239}Pu prompt fission neutron mean energies with prompt neutrons emitted between 0 and 15 MeV: DOE/NNSA CEA-DAM experimental data [5] (black symbols) are compared to JEFF3.3 [2] (red solid curve and hatched zone for 1σ uncertainties) and ENDF/B-VIII.0 [7] (blue dashed curve) libraries.

the multichance fission cross sections. Indeed, up to an energy of 5 MeV, prompt fission neutrons are only emitted by the fission fragments following a Maxwellian spectrum. With the opening of the second-chance fission, two types of neutron spectra mix: the prompt fission neutrons of the plutonium isotopes (240 and 239) emitted by the fragments following a Maxwellian spectrum with a mean energy of about 2 MeV and the neutrons emitted before fission by the ^{239}Pu compound nucleus with a mean energy evaporation spectrum of a few hundred keV.

The experimental mean energies of prompt fission neutrons are compared in Fig. 1 with those from the European JEFF3.3 [2] (red solid curve) and American ENDF/B-VIII.0 [7] (blue dashed curve) libraries, both calculated between 0 and 15 MeV. The JEFF3.3 mean energy (evaluated with uncertainties by our team) slightly underestimates the measurements up to 5 MeV. Between 5 and 20 MeV, the JEFF3.3 values describe the mean energy minima but they are too pronounced to reproduce the experimental data. From 25 to 30 MeV the data from the JEFF3.3 library are in agreement with the measurements. When we looked for the parameters of the Madland-Nix model to represent the prompt fission neutron spectra and multiplicities, we also estimated uncertainties on these parameters. These uncertainties increase with the fission chance number: they are of the order of 0.25% for the first-chance fission, 0.5% for the second-chance fission, and 2% for the third-chance fission. Parameter uncertainties of the Madland-Nix model are 4 and 6% for the last two chances of fission. Based on this information, we proceeded to stratified sampling of these parameters according to a normal distribution in order to calculate 1000 prompt fission

mean energies from which it is easy to estimate uncertainties. They are represented in Fig. 1 by the hatched zone. However, this uncertainty does not include those on partial fission cross sections since we only varied the parameters of the Madland-Nix model. This point will be examined in Sec. V. Regarding the mean energy of ENDF/B-VIII.0 evaluation, the calculated values are in excellent agreement with the measurements for the first few MeV and present a minimum for the second- and third-chance fissions but overestimate the first one and underestimate the second one. Moreover, this evaluation does not describe the variation of the mean energy beyond 20 MeV.

The next section will give, with the help of models, more precise values for the mean energy of neutrons emitted both by the fragments and by the compound nucleus before fission.

III. CALCULATION OF ^{239}Pu PROMPT FISSION NEUTRONS

In our paper, the neutron spectra emitted by the fission fragments are calculated using the Madland-Nix model [3]. The starting point of this model is Weisskopf's evaporation theory [8] that determines the neutron emission spectrum from a fission fragment in the center of mass referential. With a triangle excitation energy distribution of the fragment as recommended by Terrell [9] and a transformation in the laboratory system that takes into account the fragment kinetic energy, we have access to the prompt neutron spectrum of one fragment. In order to represent all the fission fragments, a fragments distribution should be taken into account. In the original Madland-Nix model, two average fragments represent this distribution, one light and one heavy. The total neutron spectrum emitted by the fission fragments φ is therefore obtained by the average of a spectrum emitted by a light fragment and by a heavy fragment. To better represent experimental spectra, this average is modified by adding a different weight for these two fragments [10]. These different weights make it possible to obtain a spectrum that is harder or softer depending on whether the weight of the light or heavy fragment is increased. We apply the weights 0.75 and 1.25 to the light and heavy fragments respectively, to produce a softer spectrum for the first- and second-chance fission. The weights are 1.5 and 0.5 for the third-fission chance and then increase until 1.75 and 0.25 for the two last fission chances. To calculate the total prompt fission neutron spectrum, the pre-fission neutron spectrum χ is added from the second-chance fission as Kornilov first pointed out [11]. This spectrum, calculated for the ^{239}Pu evaluation file with the TALYS code [12], is a composite nucleus type spectrum for incident neutron energies lower than 10 MeV with a preequilibrium neutron component for higher energies.

The total prompt fission neutron spectrum Φ is, therefore, the sum of the neutron spectra emitted by the fragments φ (weighted by the neutron multiplicity ν) and the pre-fission neutron spectra χ (weighted by the number of neutrons emitted before fission), both weighted by the multichance fission cross sections $\sigma_{fi} = \sigma_{n,(i-1)nf}$. The total spectrum $\Phi(E, E')$ calculated at the incident neutron energy E and the outgoing

energy E' is obtained by the sum

$$\Phi(E, E') = \frac{\sum_{i=1}^N \sigma_{fi}(E) \{ (i-1) \chi_i(E, E') + [v_i(E) - i + 1] \varphi_i(E, E') \}}{\sum_{i=1}^N \sigma_{fi}(E) \{ (i-1) \int \chi_i(E, E') dE' + [v_i(E) - i + 1] \int \varphi_i(E, E') dE' \}}. \quad (1)$$

The normalized spectra φ_i and the multiplicities v_i are therefore calculated with the Madland-Nix model while the multichance fission cross sections σ_{fi} as well as the normalized prefission spectra χ_i (suggested by Maslov [13]) are obtained with the Hauser-Feshbach formalism [4] using the TALYS code. Both models include numerous parameters that have been adjusted to best represent the experimental quantities to produce the ^{239}Pu evaluation file for the JEFF-3.3 library. In this paper, we did not modify these parameters, which we considered as constants. Instead, we looked for multichance fission cross sections σ_{fi} , which we consider to be the only unknowns, that better reproduce prompt fission neutron measurements.

The prefission neutron mean energies calculated by the TALYS code as a function of the incident neutron energy are indicated in Fig. 2 for the second chance (n, nf) and up to the fifth chance ($n, 4nf$) by red dashed curves. The mean energy for the second-chance fission varies greatly (from around 100 keV to 12 MeV) depending on the incident neutron energy and less significantly for the higher chances. This large variation is mainly due to the preequilibrium component, which starts above about 10 MeV. In this same figure, the variations of the neutron mean energy emitted by the fragments calculated with the Madland-Nix model are also reported. These energies, which are indicated by the blue continuous curves for the five chances of fission (noted neutrons from fragments), vary little according to the incident neutron energy

(the variation is 300 keV for the first-chance fission between 1 and 30 MeV). The variations of these mean energies clearly explain the fluctuations of the total mean energy of the prompt fission neutrons: before the opening of the second-chance fission, the prompt fission neutron mean energy is of the order of 2.1 MeV (neutrons emitted by the fragments); as soon as the second chance opens, this energy must be averaged with that of the prefission neutrons which have a completely different mean energy (on the order of 100 keV at the threshold). This lowers the total mean energy of prompt fission neutrons. As the energy of the prefission neutron increases with that of the incident neutron, the total mean energy of the prompt fission neutrons increases until the opening of third-chance fission where the same phenomenon occurs. We can therefore explain the fluctuations of the prompt fission neutron energy. In the following section, we show how we can faithfully reproduce the variations of this experimental mean energy by estimating the multichance fission cross sections.

IV. ESTIMATION OF THE PARTIAL FISSION CROSS SECTIONS

To estimate partial fission cross sections, we propose two methods. The first method consists in solving a system of equations whose unknowns are the partial cross sections σ_{fi} . The second method looks for the partial fission cross sections that best reproduce the prompt fission neutron spectra and multiplicities. Both methods require knowledge of experimental and calculated prompt neutron data. It is easier to work with the moments of the distribution because it allows different equations to be written by comparing experimental and calculated moments.

The experimental moments of order n at the incident neutron energy E , $\overline{E}^{n, \text{Exp}}(E)$, are easily calculated from the experimental spectra for neutrons measured between 200 keV and 11.647 MeV. However, the uncertainty on these moments cannot be deduced correctly from the spectra because we do not have the correlations within the distribution. For the first-order moment, we have retained the uncertainty deduced from the measurement between 0 and 15 MeV (Fig. 1). For higher moments, this uncertainty is certainly greater, particularly for high incident neutron energies. Further analysis of the experiment should enable us to clarify these uncertainties.

The calculated moment of order n of the total spectrum $\Phi(E, E')$ can be written as follows, separating the terms independent from the partial cross sections σ_{fi} :

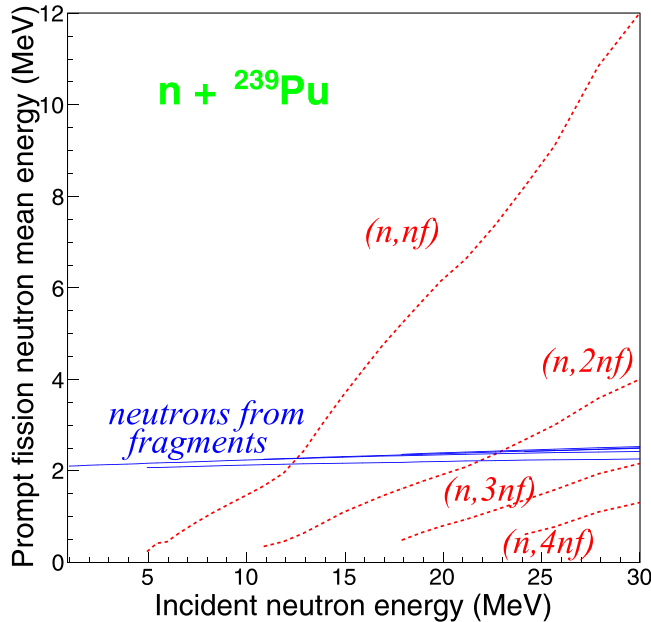


FIG. 2. Mean energies of prompt fission neutrons emitted before fission (red dashed curves) and by the fragments (blue continuous curves) for the five chances of fission.

$$\overline{E}^n(E) = \frac{\sum_{i=1}^N \sigma_{fi}(E) M_i^n(E)}{\sum_{i=1}^N \sigma_{fi}(E) L_i(E)} \quad (2)$$

with

$$M_i^n(E) = (i-1) \int E^n \chi_i(E, E') dE' + (v_i - i + 1) \int E^n \varphi_i(E, E') dE' \quad (3)$$

and

$$L_i(E) = (i-1) \int \chi_i(E, E') dE' + [v_i(E) - i + 1] \int \varphi_i(E, E') dE'. \quad (4)$$

Quantities $M_i^n(E)$ and $L_i(E)$ are calculated at the incident neutron energies E for which prompt fission neutron spectrum and multiplicity were measured. Since we have calculated the experimental moments $\overline{E}^{n, \text{Exp}}(E)$ from the experimental spectra between 200 keV and 11.647 MeV, the integrals of the previous relations are calculated over this same energy range.

A. Estimation by solving a system

If there are N multichance fissions at the incident neutron energies E , N equations are needed to determine the N partial fission cross sections $\sigma_{f_i}(E)$, $i = 1, \dots, N$. The experimental total fission cross section $\sigma_f^{\text{Exp}}(E)$, which is a fairly well-measured quantity for major actinides), provides a first equation:

$$\sum_{i=1}^N \sigma_{f_i}(E) = \sigma_f^{\text{Exp}}(E). \quad (5)$$

By writing that the $N-1$ first calculated moments $\overline{E}^n(E)$ are equal to the experimental moments $\overline{E}^{n, \text{Exp}}(E)$ (with $n = 1, \dots, N-1$), we obtain $N-1$ linear equations on partial fission cross sections:

$$\sum_{i=1}^N \sigma_{f_i}(E) [L_i(E) \overline{E}^{n, \text{Exp}}(E) - M_i^n(E)] = 0. \quad (6)$$

The experimental fission multiplicity $v^{\text{Exp}}(E)$ gives an additional equation:

$$\sum_{i=1}^N \sigma_{f_i}(E) v_i(E) = v^{\text{Exp}}(E) \sigma_f^{\text{Exp}}(E). \quad (7)$$

When only the first- and second-chance fission are open (for neutrons with an energy between approximately 5 and 10 MeV), the system of equations can be reduced to a single equation [Eq. (6) written for the first moment with $n = 1$] to determine the cross section σ_{f_1}

$$\sigma_{f_1}(E) = \frac{\sigma_f^{\text{Exp}}(E) [M_2^1(E) - L_2(E) \overline{E}^{\text{Exp}}(E)]}{\overline{E}^{\text{Exp}}(E) [L_1(E) - L_2(E)] - M_1^1(E) + M_2^1(E)} \quad (8)$$

and the second-chance fission cross section is calculated with the difference $\sigma_{f_2}(E) = \sigma_f^{\text{Exp}}(E) - \sigma_{f_1}(E)$.

We commonly use the experimental fission cross sections [Eq. (5)], the first four experimental moments [Eq. (6)], and the experimental fission multiplicity [Eq. (7)]; this allows

us to write six equations, to determine the unknown partial fission cross sections. The number of unknowns is 2 at 5 MeV and increases with energy, reaching 5 at 30 MeV. In cases where the number of unknowns is different from the number of equations, we use the Moore-Penrose inverse (pseudoinverse) [14] to determine the unknown partial fission cross sections.

Between 5 and 30 MeV, the multiplicities and spectra are measured for 24 incident neutron energies. For each energy E_j , we compute the $v_i(E_j)$, $M_i^n(E_j)$ and $L_i(E_j)$ terms (with $n = 1, \dots, 4$ and $i = 1, \dots, N_j$ where N_j is the number of multichance fission cross sections at energy E_j) from the Madland-Nix and Hauser-Feshbach models. Then the partial fission cross sections are calculated thanks to the pseudoinverse. A system of six equations is first used to determine a solution. Other solutions are found by reducing the number of equations [for example Eqs. (5) and (7) or Eqs. (5) and (6) with $n = 1, 2, \dots$]. The pseudoinverse method can lead to negative solutions and this happens especially at partial fission cross-section thresholds. To overcome this problem, we use the following method: if one partial fission cross section is found between -50 mb and 0, it is counted as zero, the sum is normalized to the experimental fission cross section, and this solution is retained; if the cross section is less than -50 mb, this solution is not considered relevant for defining partial fission cross sections. This eliminates solutions with cross sections lower than -50 mb and retains those with cross sections between -50 and 0 mb.

We thus obtain, for each energy, several sets of solutions that can be averaged and from which we are able to calculate a standard deviation. The partial fission cross sections are represented in Fig. 3 by stars with the uncertainty due to the method. For certain energies, particularly at the threshold and beyond 20 MeV, the uncertainty is very large. In this case, it is not shown so that the figure remains readable.

Since this method does not allow us to obtain accurate cross sections in all the energy range (especially above 20 MeV) we tried to obtain them with a second method.

B. Estimation by variation

For this method, called the variation of partial fission cross sections, we used the ^{239}Pu partial fission cross sections previously calculated for the JEFF3.3 library as a starting point. Then, simply vary the partial fission cross sections around the starting values [while preserving equality (5)] and keep those that most faithfully reproduce the measurements of moments and multiplicities. The selected cross sections are those with the smallest relative difference between the calculated and experimental data. To calculate this relative difference, a weight is assigned to each observable: 0.3 for the multiplicity, 0.4 for the first-order moment, and 0.2 for the second-order moment. The last two moments are assigned a weight of 0.05.

This method has the disadvantage of giving discontinuous cross sections. To avoid abrupt changes in fission cross sections, we have added constraints on the variations of the first- and second-chance fission: the first-chance fission cross section must not include any abrupt changes and must decrease when the incident neutron energy increases, while the

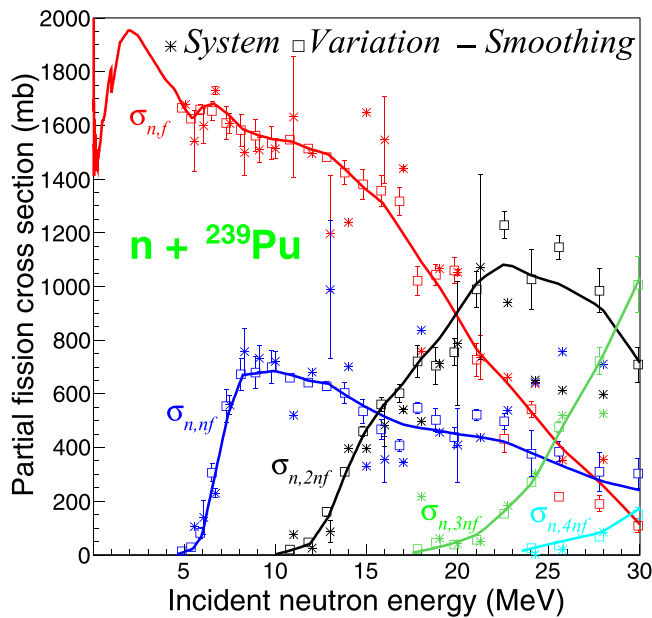


FIG. 3. Partial fission cross sections obtained by solving a system of equations (indicated by stars), searching for the values that best reproduce the experimental moments as well as multiplicities (marked by squares) and finally smoothed from the previous results (full lines). The colors show the multichance fission cross sections (denoted $\sigma_{n,f}$ in red, $\sigma_{n,nf}$ in blue, $\sigma_{n,2nf}$ in black, $\sigma_{n,3nf}$ in green, and $\sigma_{n,4nf}$ in cyan).

second-chance fission cross section must decrease when the third-chance fission opens (above 10 MeV). To estimate the uncertainties obtained with this method, we retain for each incident energy the first 100 multichance fission cross sections that best reproduce the experimental moments and multiplicity. From these values, we then obtain the uncertainties on this method. The standard deviation is of the order of 5% for energies below 10 MeV, and decreases sharply for certain energy ranges, e.g., around 12 and 17 MeV. The results obtained with the variation method are represented in Fig. 3 by different color squares according to the multichance fission cross section. These new results are in agreement with the first method up to 10-MeV energy and comprise many fewer fluctuations thanks to the imposed constraints.

C. Smoothing

By smoothing the results of the two previous methods, we have estimated new partial fission cross sections for the ^{239}Pu . These cross sections are also indicated in Fig. 3 by continuous curves. These values with their standard deviations calculated by averaging the standard deviations of the system and variation methods are represented by the red curves with hatched areas in Fig. 4. They are compared with those calculated for the JEFF3.3 library (blue curves). These cross sections are very different, especially for first- and second-chance fission. The second-chance fission cross section is greatly reduced in favor of the first-chance fission cross section, in order to increase the mean energy of prompt fission neutrons. Let us also recall that the total fission cross section (red curve on the upper part

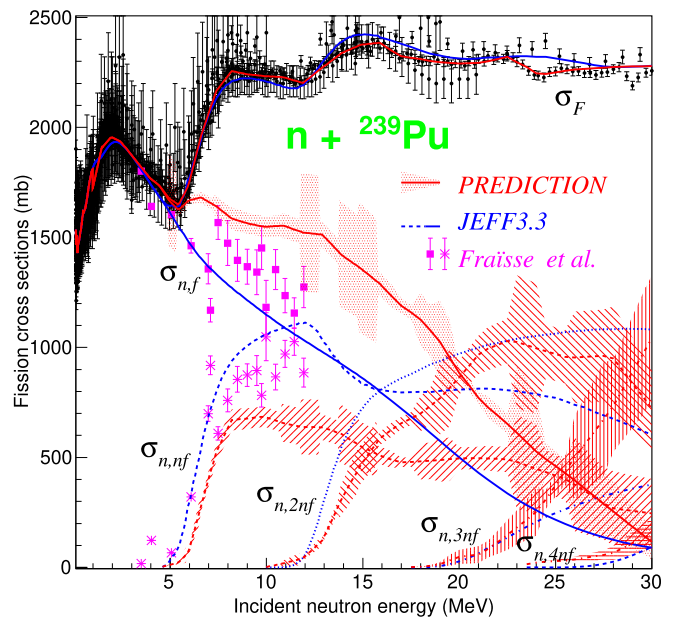


FIG. 4. Partial fission cross sections were obtained after smoothing the results of the system and variation methods (red curves with hatched areas). These values are compared with those obtained by Fraïsse *et al.* [1] ($\sigma_{n,f}$ magenta squares and $\sigma_{n,nf}$ magenta stars) and with the JEFF3.3 evaluation (blue curves without hatched areas). The experimental data for the total fission cross section are taken from the EXFOR database [15–18].

of Fig. 4) has been slightly modified by trying to faithfully reproduce the experimental fission cross section. When the JEFF library will be reviewed, we will have to see whether it is possible to obtain partial fission cross sections of this type with the models that we currently use to construct the plutonium evaluation.

Figure 4 also shows the indirect measurements of Fraïsse *et al.* [1]. Magenta squares represent first-chance fission, while magenta stars indicate second-chance fission. These measurements lie between our estimates of partial fission cross sections and those from JEFF3.3. They do not allow us to decide in favor of one result or the other.

We can also provide advice on the ENDF/B-VIII.0 ^{239}Pu partial fission cross sections if we assume that the Madland-Nix model and the Hauser-Feshbach formalism are used in a similar way to build this evaluation. Referring to Fig. 1, we can say that the second-chance fission cross section is probably not large enough between 5 and 11 MeV and that the third-chance fission cross section is too large between 12 and 16 MeV. We are unable to verify this opinion as unfortunately the new evaluations no longer contain this information.

Not only do we have an estimate of the partial fission cross sections, but we can now reproduce even better the mean energies, spectra, and multiplicities of the prompt fission neutrons as we shall see in Sec. V.

V. COMPARISONS WITH JEFF3.3

In this last section, we propose to compare the mean energy, the multiplicities, and the spectra of prompt fission

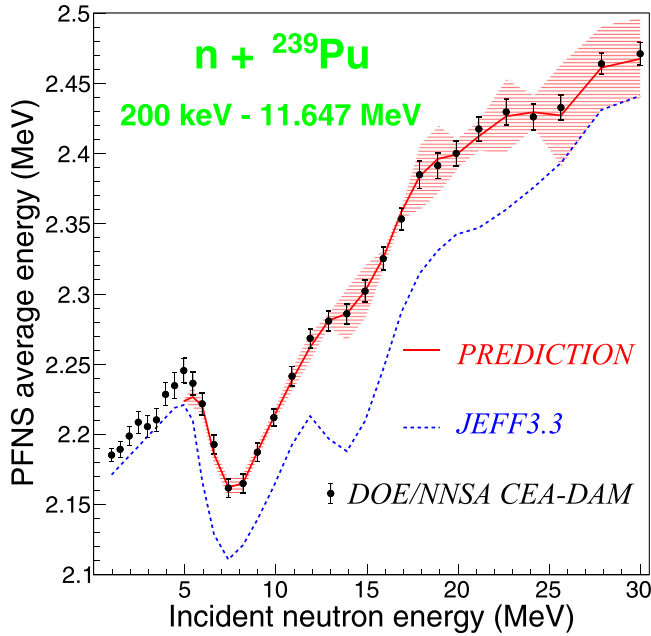


FIG. 5. Prompt fission neutron mean energy calculated with the new partial fission cross sections (red curve with hatched zone) compared with that obtained with the JEFF3.3 cross sections (blue dotted curve). The DOE/NNSA CEA-DAM measurements [5] are indicated by the black dots with their error bar. The mean energy is calculated between 200 keV and 11.647 MeV, the neutron detection energy limits.

neutrons calculated using our new partial fission cross sections with the values that we have evaluated for the European library JEFF3.3.

Since we have estimated the multichance fission cross sections' uncertainties, we propagate this information to the mean energies and multiplicities. So, for each incident energy, we constructed 1000 sets of partial fission cross sections sampled according to normal distributions with mean and standard deviation shown in Fig. 4. These sampled partial cross sections are then normalized to the experimental total fission cross section. For each set, we calculate the average energy and multiplicity of prompt fission neutrons and then estimate a standard deviation for these quantities.

A. Mean energy

Figure 5 shows the variations of the prompt fission neutron mean energy calculated from the estimation of the partial fission cross sections (red curves). One sigma uncertainty due to cross sections' uncertainties is represented by the hatched areas. They are compared with those obtained from the JEFF3.3 library cross (blue dotted curve). The measurements, calculated from the DOE/NNSA CEA-DAM experimental spectra [5], are indicated by the black dots with their error bar. All these results are averaged over the 200-keV to 11.647-MeV energy range. This estimation therefore makes it possible to perfectly reproduce the experimental value between 5 and 30 MeV. When only first-chance fission is present, the calculated energy slightly underestimates

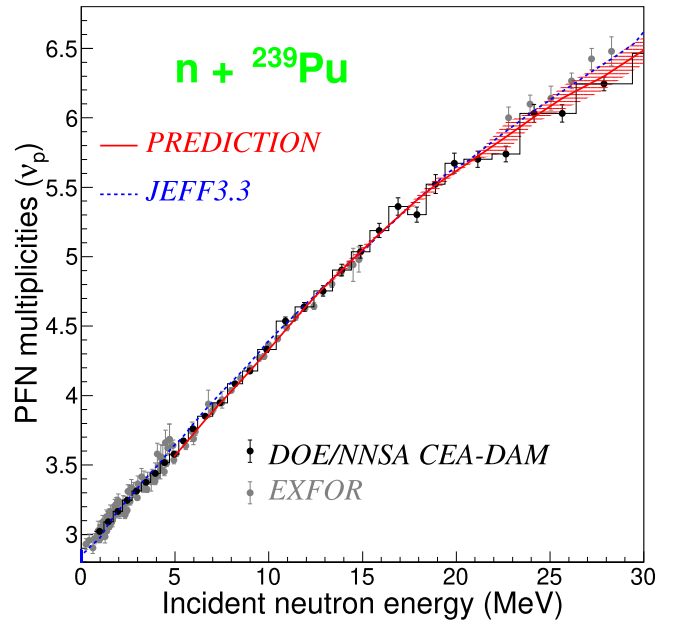


FIG. 6. Prompt fission neutron multiplicities calculated with the new partial fission cross sections (red curve with hatched zone) compared with those from the JEFF3.3 library (blue dotted curves). The measurements taken by the DOE/NNSA CEA-DAM collaboration [6] are reported in black while those extracted from EXFOR are from Refs. [19–23].

the measurement by about 0.5%. It should be possible to reduce this calculation-experiment disagreement by slightly modifying the parameters of the Madland-Nix model for the first chance. This modification will be carried out with our new partial fission cross sections in a future work. The JEFF3.3 mean energy has a too marked first-chance minimum and a much too pronounced second-chance minimum. Above 5 MeV, the mean energy calculated with the JEFF3.3 cross sections is much too low.

B. Multiplicities

Recent measurements of the prompt fission neutron multiplicities from the DOE/NNSA CEA-DAM collaboration [6] are represented in Fig. 6 by the black dots and those older by the gray dots (taken from EXFOR [24] from Refs. [19–23]). They are compared with the multiplicities calculated with the new partial fission cross sections (red curve) and represented with one sigma uncertainty due to cross sections' uncertainties (red hatched areas). Those from the JEFF3.3 evaluation are indicated by the blue dotted curve. For incident neutron energy lower than 15 MeV or higher than 25 MeV, the new cross sections lead to multiplicities in better agreement with experiment. Note however that for the JEFF3.3 evaluation, we slightly adjusted the multiplicity between 1 keV and 10 MeV to better reproduce the criticality benchmarks. It will therefore be necessary to ensure that this new multiplicity makes it possible to correctly describe the critical experiments.

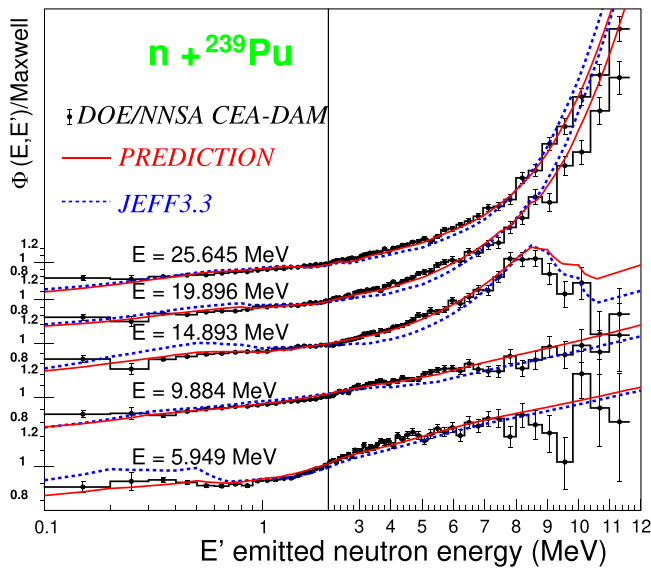


FIG. 7. Prompt fission neutron spectra referred to the Maxwellian spectrum ($T = 1.32$ MeV) for incident energies of 5.949, 9.884, 14.893, 19.896, and 25.645 MeV. The experiment is indicated by the black curve (DOE/NNSA CEA-DAM [5]). The red curves show the spectra calculated with the new partial fission cross sections and are also compared to the spectra from the JEFF3.3 library (dotted blue curves).

C. Spectra

Between 5 and 30 MeV, we chose five incident neutron energies among the 24 measured energies to represent the prompt fission neutron spectra: 5.949, 9.884, 14.893, 19.896, and 25.645 MeV. Since the shape of fission spectra can be roughly approximated by a Maxwellian spectrum, it is customary to represent these spectra relative to a Maxwellian spectrum. This representation, which makes it possible to highlight the differences between the calculations and the measurements in the entire energy range of emitted neutrons, has been adopted in Fig. 7 assuming a Maxwell temperature T of 1.32 MeV.

The spectra calculated with the new estimation of the partial fission cross sections are indicated by the red curves in Fig. 7. These results are in excellent agreement with the measurements represented by the black symbols, particularly in the energy range 100 keV to 8 MeV which corresponds to

the peak of the prompt neutron emission spectrum. In the same figure, the spectra we had evaluated for the JEFF3.3 library are represented by the blue dotted curves. It should be noted that this evaluation had been carried out before these new prompt fission neutron spectra measurements. The recent description of the spectra represents the experiment much better, thanks to the new partial fission cross sections.

VI. CONCLUSION

We have estimated partial fission cross sections of the plutonium 239 nucleus for the first time between 5 and 30 MeV. This estimate is essentially based on the precise measurements of the prompt fission neutron spectra and multiplicities as well as on the Madland-Nix model and Hauser-Feshbach formalism. We have retained the parameters determined for the ^{239}Pu JEFF-3.3 evaluation file, both for the neutrons emitted by the fragments (Madland-Nix) and before fission (Hauser-Feshbach). Thus, questioning the experimental results or a component of these models could modify the estimation of these cross sections.

These new partial cross sections, which reproduce the measurements much better than those calculated for the last evaluation of the JEFF3.3 library, can be proposed for future evaluations.

These partial cross sections should also serve as a guide for determining the future total fission cross section of the next JEFF library. It remains to be seen whether the models we use to build an evaluation are able to reproduce these partial fission cross sections while correctly predicting the other parts of the evaluation.

Since there is a slight disagreement on the mean energy for incident neutrons of energy less than 5 MeV, a new iteration of the search for the parameters of the Madland-Nix model is necessary. This will have to be carried out using the partial fission cross sections determined for the next ^{239}Pu evaluation, for which our predictions on the partial fission cross sections will have served as a guide. By reestimating the fission cross sections with the new Madland-Nix parameters, we could get an idea of the sensitivity of this estimate to Madland-Nix parameters.

The method for determining partial fission cross sections for ^{239}Pu could also be used for 235 and 238 uranium isotopes, since experiments have been carried out by the DOE/NNSA CEA-DAM collaboration for these actinides.

- [1] B. Fraïsse, G. Bélier, V. Méot, L. Gaudefroy, A. Francheteau, and O. Roig, *Phys. Rev. C* **108**, 014610 (2023).
- [2] A. J. M. Plompen, O. Cabellos, C. De Saint Jean, M. Fleming, A. Algora, M. Angelone, P. Archier, E. Bauge, O. Bersillon, A. Blokhin *et al.*, *Eur. Phys. J. A* **56**, 181 (2020).
- [3] D. G. Madland and J. R. Nix, *Nucl. Sci. Eng.* **81**, 213 (1982).
- [4] W. Hauser and H. Feshbach, *Phys. Rev.* **87**, 366 (1952).
- [5] P. Marini, J. Taieb, B. Laurent, G. Belier, A. Chatillon, D. Etasse, P. Morfouace, M. Devlin, J. A. Gomez, R. C. Haight *et al.*, *Phys. Rev. C* **101**, 044614 (2020).
- [6] P. Marini, J. Taieb, D. Neudecker, G. Blier, A. Chatillon, D. Etasse, B. Laurent, P. Morfouace, B. Morillon, M. Devlin *et al.*, *Phys. Lett. B* **835**, 137513 (2022).
- [7] D. A. Brown, M. B. Chadwick, R. Capote, A. C. Kahler, A. Trkov, M. W. Herman, A. A. Sonzogni, Y. Danon, A. D. Carlson, M. Dunn *et al.*, *Nucl. Data Sheets* **148**, 1 (2018).
- [8] J. M. Blatt and V. F. Weisskopf, *Theoretical Nuclear Physics* (Dover, New York, 1991).
- [9] J. Terrell, *Phys. Rev.* **113**, 527 (1959).
- [10] R. Capote, Chen Y.-J., F.-J. Hamsch, N. V. Kornilov, J. P. Lestone, O. Litaize, B. Morillon, D. Neudecker,

- S. Oberstedt, T. Ohsawa *et al.*, *Nucl. Data Sheets* **131**, 1 (2016).
- [11] N. V. Kornilov, Translation of selected papers published in *Yadernye Konstanty*, Nuclear Constants Issue No. 4 (1985), INDC(CCP)-336 (1991).
- [12] A. J. Koning, S. Hilaire, and S. Goriely, *Eur. Phys. J. A* **59**, 131 (2023).
- [13] V. M. Maslov, Y. V. Porodzinskij, M. Baba, A. Hasegawa, N. V. Kornilov, A. B. Kagalenko, and N. A. Tetereva, *Phys. Rev. C* **69**, 034607 (2004).
- [14] R. Penrose, *Math. Proc. Camb. Phil. Soc.* **51**, 406 (1955).
- [15] F. Tovesson and T. S. Hill, *Nucl. Sci. Eng.* **165**, 224 (2010), EXFOR 14271.
- [16] O. Shcherbakov, A. Donets, A. Evdokimov, A. Fomichev, T. Fukahori, A. Hasegawa, A. Laptev, V. Maslov, G. Petrov, S. Soloviev *et al.*, *J. Nucl. Sci. Technol.* **39**(Suppl. 2), 230 (2002), EXFOR 41455.
- [17] J. W. Meadows, *Nucl. Sci. Eng.* **68**, 360 (1978), EXFOR 10734.
- [18] K. Kari, Kernforschungszentrum Karlsruhe Reports, No. 2673 (1978), EXFOR 20786.
- [19] J. C. Hopkins and B. C. Diven, *Nucl. Phys.* **48**, 433 (1963), EXFOR 12326.
- [20] H. Conde, J. Hansen, and M. Holmberg, *J. Nucl. Energy* **22**, 53 (1968), EXFOR 20052.
- [21] M. V. Savin, Y. A. Khokhlov, Y. S. Zamyatin, and I. N. Paramonova, Nucl. Data Reactors Conf., Helsinki **2**, 157 (1970), EXFOR 40058.
- [22] B. Nurpeisov, K. E. Volodin, V. G. Nesterov, L. I. Prokhorova, G. N. Smirenkin, and Yu. N. Turchin, *Sov. At. Energy* **39**, 807 (1975), EXFOR 40429.
- [23] M. Soleilhac, J. Frehaut, and J. Gauriau, *J. Nucl. Energy* **23**, 257 (1969), EXFOR 20490.
- [24] EXchange FORmat database (EXFOR) is maintained by the Network of Nuclear Reaction Data Centers (see www-nds.iaea.org/nrdc/). Data are available online (e.g., at www-nds.iaea.org/exfor/).